N91-17074

COMPARISON OF TWO ON-ORBIT ATTITUDE SENSOR ALIGNMENT METHODS

Kenneth Krack and Michael Lambertson
Computer Sciences Corporation
10110 Aerospace Road
Lanham-Seabrook, MD 20706

and

F. Landis Markley
National Aeronautics and Space Administration (NASA)
Goddard Space Flight Center
Greenbelt, MD 20771

Abstract

This paper compares two methods of on-orbit alignment of vector attitude sensors. The first method uses the angular difference between simultaneous measurements from two or more sensors. These angles are compared to the angular differences between the respective reference positions of the sensed objects. The alignments of the sensors are adjusted to minimize the difference between the two sets of angles. In the second method, the sensor alignment is part of a state vector that includes the attitude. The alignments are adjusted along with the attitude to minimize all observation residuals. It is shown that the latter method can result in much less alignment uncertainty when gyroscopes are used for attitude propagation during the alignment estimation. The additional information for this increased accuracy comes from knowledge of relative attitude obtained from the spacecraft gyroscopes. This paper presents the theoretical calculations of this difference in accuracy. Also presented are numerical estimates of the alignment uncertainties of the fixed-head star trackers on the Extreme Ultraviolet Explorer spacecraft using both methods.

1. INTRODUCTION

This paper compares two methods of determining the in-flight alignment estimation of vector-type attitude sensors. The two methods of alignment estimation will be referred to as attitude-independent and attitude-dependent and are outlined below. The estimated accuracy of the two approaches will be discussed.

Vector-type attitude sensors are those sensors whose output are vector measurements of the lines-of-sight to some reference object. Examples of this type of sensor are Sun sensors and star trackers. A minimum of two vector observations are needed for attitude determination. The analysis presented in this paper will be restricted to observations from two fixed-head star trackers (FHSTs) for simplicity.

Section 2 discusses the theoretical differences in the accuracy of these two approaches. Section 3 presents a numerical example of both methods using the Extreme Ultraviolet Explorer (EUVE) spacecraft as a typical mission case.

ATTITUDE-INDEPENDENT ALIGNMENT ESTIMATION

The attitude-independent method of sensor alignment estimation discussed here is based on an algorithm first presented in a paper by Shuster, Chitre, and Niebur (Reference 1) and later refined by Bierman and Shuster (Reference 2). This method of sensor alignment estimation uses the angle between two vector observations as its basic observation. This scalar observation is compared to the angle between the corresponding reference objects, and the sensor alignment is adjusted to minimize the difference. The method requires simultaneous measurements in each sensor. No a priori knowledge of the attitude is used nor does the algorithm solve for the attitude. The algorithm seeks to minimize the overall deviation of the sensor alignments from their prelaunch values.

ATTITUDE-DEPENDENT ALIGNMENT ESTIMATION

In an attitude-dependent alignment estimation method, the spacecraft attitude is part of a state vector that includes the sensor alignments. The attitude is either solved-for along with the alignment or is treated as a known quantity. The primary observation quantity is the unit vector measurement from the sensors as opposed to the scalar measurement of the attitude-independent

method. Residuals are computed between estimated observations based on the state vector and the actual observations. The state vector is adjusted to minimize the residuals. Two procedures are in common use to obtain this minimization: the sequential filter and the batch filter. The sequential filter updates its estimation of the state vector at discrete times using a previously estimated state that has been propagated from the time of the last sensor observation. The batch filter considers a collection of sensor observations in toto and seeks to minimize all residuals simultaneously. Both procedures require knowledge of the motion of the spacecraft between observations. This knowledge is usually obtained from gyroscope measurements but could be inferred from a dynamics model of the spacecraft. The analysis in this paper will restrict itself to the batch filter and will assume dynamics information is available.

2. THEORETICAL EVALUATION

As stated in the introduction, this analysis will assume a spacecraft with two FHSTs. The state vector (References 3 through 5) to be estimated is

$$\bar{x}(t) = \begin{bmatrix} \Delta\vec{\theta}(t) \\ \vec{m}_1 \\ \vec{m}_2 \end{bmatrix}$$

where $\Delta\vec{\theta}(t)$ is a vector of attitude error angles around the spacecraft body axes and $\vec{m}_i$ (for i = 1 and 2) is a vector of sensor misalignment angles around the i^{th} FHST axes (References 4 and 5).

A batch least-squares estimate of the state at an epoch time t_o, ignoring the effects of dynamics noise and consider parameters, has the covariance (Reference 3)

$$P(t_o) \equiv E\left[\bar{x}(t_o)\, \bar{x}^T(t_o) \right] = W_n^{-1}$$

where W_n is the normal matrix,

$$W_n = W_o + F^T W F$$

This quantity contains attitude information. For simplicity, assume the sensor alignments, B_1 and B_2, are given by

$$B_1 = I_{3x3} = 3 \times 3 \text{ identity matrix}$$

$$B_2 = \begin{bmatrix} 0 & 0 & -1 \\ 0 & 1 & 0 \\ 1 & 0 & 0 \end{bmatrix} = \text{rotation by 90 degrees (deg) about the y-axis}$$

Thus, the sensor boresight, which is along the z-axis in the sensor frame, is along the spacecraft z- and x-axis for FHST-1 and FHST-2, respectively. The partial derivatives of the observations with respect to the state vector components are needed to compute the normal matrix. Again for simplicity, assume the observed stars are on the sensor boresights. The partial derivative matrix for the scalar observation is

$$G_s \equiv \frac{\partial s}{\partial \bar{x}} = \left[0_{1x3}, \ (\hat{W}_1 \times B_1 B_2^T \hat{W}_2)^T, \ (\hat{W}_2 \times B_2 B_1^T \hat{W}_1)^T \right]$$

$$= [\ 0,\ 0,\ 0,\ 0,\ 1,\ 0,\ 0,\ -1,\ 0\ ]$$

For the assumed geometry, the variance of the errors in the scalar observation, s, is $2\sigma_m^2$. The partial derivative matrix for the vector observation is (References 4 and 5)

$$G_v \equiv \frac{\partial \bar{y}}{\partial \bar{x}} = \left[\begin{array}{c|c|c} M & M & 0_{2x3} \\ \hline MB_2 & 0_{2x3} & M \end{array} \right]$$

where

$$M = \begin{bmatrix} 0 & 1 & 0 \\ -1 & 0 & 0 \end{bmatrix}$$

The attitude and misalignment variances will be computed for four cases. For either a scalar or vector observation type, either a single measurement or else two measurements separated by a 90-deg attitude maneuver about the space-

The matrix W_o is the inverse of the a priori covariance of $\bar{x}$ and $F^T W F$ represents the information contained in the measurements. Assuming no a priori attitude knowledge and a priori knowledge of sensor misalignments with standard deviation σ_a per axis gives

$$W_o = \sigma_a^{-2} \left[\begin{array}{c|c} 0_{3x3} & 0_{3x6} \\ \hline 0_{3x6} & I_{6x6} \end{array} \right]$$

where 0_{nxm} denotes an n x m matrix of zeros and I_{nxn} is an n x n identity matrix. The form of the matrices F and W depends on the measurements.

The i^{th} FHST returns the two-component measurement

$$\bar{Z}_i = -\begin{bmatrix} W_{ix} / W_{iz} \\ W_{iy} / W_{iz} \end{bmatrix}$$

where $\hat{W}_i$ is the unit vector measurement of the star in FHST coordinates (References 4 and 5). The errors in the two components of $\bar{Z}_i$ are assumed to be uncorrelated and to have equal measurement variances denoted by σ_m^2.

The observation at a given time processed by the estimator is a function of $\bar{Z}_1$ and $\bar{Z}_2$. The attitude-independent observation is a scalar given by the inner product of the two star vectors in the spacecraft body frame.

$$s = \hat{W}_1^T B_1 B_2^T \hat{W}_2$$

where B_1 and B_2 are the sensor alignment matrices that rotate a vector from the spacecraft body frame to FHST-1 and FHST-2 frames, respectively. This quantity contains no attitude information.

The attitude-dependent observation is a four-component vector

$$\bar{y} = \begin{bmatrix} \bar{Z}_1 \\ \bar{Z}_2 \end{bmatrix}$$

craft y-axis will be considered. The estimate epoch time will be taken to be the time of the first observation. The measurement weight matrix, W, will be assumed to be the inverse of the measurement covariance in all cases. The measurement error propagation matrix between the two observation times is given by (References 3 through 5)

$$\Phi = \left[\begin{array}{c|c} \Phi_\theta & 0_{3x6} \\ \hline 0_{6x3} & I_{6x6} \end{array}\right]$$

where Φ_θ represents a 90-deg rotation about the y-axis. The four measurement scenarios and their associated weight and total derivative matrices follow:

1. A single scalar observation

$$F = G_s$$

$$W = \frac{1}{2}\sigma_m^{-2}$$

2. Two scalar observations separated by a 90-deg maneuver

$$F = \begin{bmatrix} G_s \\ G_s \Phi \end{bmatrix}$$

$$W = \frac{1}{2}\sigma_m^{-2} I_{2x2}$$

3. A single four-vector observation

$$F = G_v$$

$$W = \sigma_m^{-2} I_{4x4}$$

4. Two four-vector observations separated by a 90-deg maneuver

$$F = \begin{bmatrix} G_v \\ G_v \Phi \end{bmatrix}$$

$$W = \sigma_m^{-2} I_{8x8}$$

For each scenario the normal matrix will be computed and then inverted to obtain the covariance matrix. In all cases a permutation of the rows and

columns of the normal matrix will bring it to block diagonal form, facilitating matrix inversion. This permutation corresponds to rearranging the state vector as

$$\bar{x}' \equiv \left[\Delta\theta_x,\ m_{1x},\ \Delta\theta_z,\ m_{2x},\ \Delta\theta_y,\ m_{1y},\ m_{2y},\ m_{1z},\ m_{2z} \right]^T$$

The normal matrix with the permuted rows and columns will similarly be distinguished by a prime, W_n'.

SCENARIO 1: A SINGLE SCALAR OBSERVATION

First consider scenario 1, a single scalar observation, for which

$$F^T W\ F = \frac{1}{2}\,\sigma_m^{-2}\,G_s^T G_s = \frac{1}{2}\,\sigma_m^{-2} \left[\begin{array}{c|c|c} 0_{3x3} & 0_{3x3} & 0_{3x3} \\ \hline 0_{3x3} & D & -D \\ \hline 0_{3x3} & -D & D \end{array}\right]$$

where D = diag(0, 1, 0) and diag(...) denotes a diagonal matrix with the indicated elements along the diagonal. The permuted normal matrix in this scenario is

$$W_n' = \sigma_m^{-2} \left[\begin{array}{ccccccccc} 0 & & & & & & & & \\ & \alpha & & & & & & & \\ & & 0 & & & & & & \\ & & & \alpha & & & & & \\ & & & & 0 & & & & \\ & & & & & (\alpha + 1/2) & -1/2 & & \\ & & & & & -1/2 & (\alpha + 1/2) & & \\ & & & & & & & \alpha & \\ & & & & & & & & \alpha \end{array}\right]$$

where

$$\alpha = (\sigma_m\ /\ \sigma_a)^2$$

These variances, however, have the same limits for $\sigma_m \gg \sigma_a$ and $\sigma_m \ll \sigma_a$ as in scenario 1.

SCENARIO 3: A SINGLE FOUR-VECTOR OBSERVATION

Scenario 3, a single four-vector observation, gives

$$F^T W F = \sigma_m^{-2} G_v^T G_v = \sigma_m^{-2} \left[\begin{array}{c|c} \Gamma_{\theta\theta} & \Gamma_{\theta m} \\ \hline \Gamma_{\theta m}^T & \Gamma_{mm} \end{array}\right]$$

where

$$\Gamma_{\theta\theta} = \mathrm{diag}(1,\ 2,\ 1)$$

$$\Gamma_{\theta m} = \begin{bmatrix} 1 & 0 & 0 & 0 & 0 & 0 \\ 0 & 1 & 0 & 0 & 1 & 0 \\ 0 & 0 & 0 & -1 & 0 & 0 \end{bmatrix}$$

$$\Gamma_{mm} = \mathrm{diag}(1,\ 1,\ 0,\ 1,\ 1,\ 0)$$

The permuted normal matrix is

$$W'_n = \sigma_m^{-2} \left[\begin{array}{cc|cc|ccc|c|c} 1 & 1 & & & & & & & \\ 1 & (\alpha+1) & & & & & & & \\ \hline & & 1 & -1 & & & & & \\ & & -1 & (\alpha+1) & & & & & \\ \hline & & & & 2 & 1 & 1 & & \\ & & & & 1 & (\alpha+1) & 0 & & \\ & & & & 1 & 0 & (\alpha+1) & & \\ \hline & & & & & & & \alpha & \\ \hline & & & & & & & & \alpha \end{array}\right]$$

Inverting this matrix gives the attitude variances

The variances of the state vector components are the diagonal elements of the inverse of W'_n. Thus, in this scenario the attitude error variances are all infinite, which is to be expected with attitude-independent observations. The four misalignment variances, $\sigma^2(m_{1x})$, $\sigma^2(m_{1z})$, $\sigma^2(m_{2x})$, and $\sigma^2(m_{2z})$, are all equal to their a priori values, σ_a^2, which means that the single scalar observation does not contain information about these misalignments. The y component of the misalignment variances for each of the two sensors is given by

$$\sigma^2(m_{1y}) = \sigma_a^2 \left(\frac{\sigma_m^2 + 1/2\ \sigma_a^2}{\sigma_m^2 + \sigma_a^2} \right)$$

It is instructive to examine two limiting cases: the case of sensor data uncertainty much less than the a priori state vector uncertainty ($\sigma_m \ll \sigma_a$) and the opposite case of poor measurement accuracy ($\sigma_m \gg \sigma_a$). The y-axis alignment variance for scenario 1 has the limit σ_a^2 for $\sigma_m \gg \sigma_a$ and $(1/2)\ \sigma_a^2$ for $\sigma_m \ll \sigma_a$. The former result is reasonable since the measurements do not improve the a priori estimates in this limit. In the opposite limit of accurate measurements, the y-axis misalignments of the two FHSTs are in some sense averaged. These results are independent of the number of observations.

SCENARIO 2: TWO SCALAR OBSERVATIONS SEPARATED BY A MANEUVER

For scenario 2, two scalar observations separated by a 90-deg maneuver,

$$F^T W F = \frac{1}{2}\ \sigma_m^{-2} \left(G_s^T G_s + \Phi^T G_s^T G_s \Phi \right) = \sigma_m^{-2}\ G_s^T G_s$$

since it is easily seen that

$$\Phi^T G_s^T G_s \Phi = G_s^T G_s$$

Thus, the only change in W'_n from scenario 1 is to replace each 1/2 in the matrix by 1, and the only variances that are modified are

$$\sigma^2(m_{1y}) = \sigma_a^2 \left(\frac{\sigma_m^2 + \sigma_a^2}{\sigma_m^2 + 2\ \sigma_a^2} \right)$$

$$\sigma^2(\Delta\theta_x) = \sigma^2(\Delta\theta_z) = \sigma_a^2 + \sigma_m^2$$

$$\sigma^2(\Delta\theta_y) = \frac{1}{2}\left(\sigma_a^2 + \sigma_m^2\right)$$

These results can be understood intuitively as follows. An observation of a star on the boresight of FHST-1, which is aligned with the spacecraft z-axis, provides information about the x- and y-axis attitude errors. Similarly, an observation of a star on the boresight of FHST-2, which is aligned with the spacecraft x-axis, provides information about the y- and z-axis attitude errors. As there is twice as much information about the y-axis attitude, the variance of the y-axis attitude is half as large as that of the other two axes. The x- and z-axis uncertainties are the root-sum-square of the a priori alignment uncertainty and the measurement uncertainty.

The alignment variances are the same as in scenario 1; therefore, no alignment information is lost or gained by combining the four components of the vector observations into a single scalar observation for measurements taken at a single attitude.

SCENARIO 4: TWO FOUR-VECTOR OBSERVATIONS SEPARATED BY A MANEUVER

The final scenario, two four-vector observations separated by a 90-deg maneuver, has

$$F^T W F = \sigma_m^{-2}\left(G_v^T G_v + \Phi^T G_v^T G_v \Phi\right)$$

where

$$\Phi^T G_v^T G_v \Phi = \left[\begin{array}{c|c} \Phi_\theta^T \Gamma_{\theta\theta} \Phi_\theta & \Phi_\theta^T \Gamma_{\theta m} \\ \hline \Gamma_{\theta m}^T \Phi_\theta & \Gamma_{mm} \end{array}\right]$$

It is easy to see that

$$\Phi_\theta^T \Gamma_{\theta\theta} \Phi_\theta = \Gamma_{\theta\theta}$$

however,

$$\Phi_\theta^T \Gamma_{\theta_m} = \begin{bmatrix} 0 & 0 & 0 & -1 & 0 & 0 \\ 0 & 1 & 0 & 0 & 1 & 0 \\ -1 & 0 & 0 & 0 & 0 & 0 \end{bmatrix} \neq \Gamma_{\theta_m}$$

Thus, in contrast to the scalar observation case, the structure of the normal matrix will be different when a spacecraft maneuver is performed during alignment. The normal matrix is

$$W'_n = \sigma_m^{-2} \begin{bmatrix} \begin{vmatrix} 2 & 1 & 0 & -1 \\ 1 & (\alpha+2) & -1 & 0 \\ 0 & -1 & 2 & -1 \\ -1 & 0 & -1 & (\alpha+2) \end{vmatrix} & 0 \\ 0 & \begin{vmatrix} 4 & 2 & 2 \\ 2 & (\alpha+2) & 0 \\ 2 & 0 & (\alpha+2) \end{vmatrix} \\ & \begin{vmatrix} \alpha & \\ & \alpha \end{vmatrix} \end{bmatrix}$$

It can be seen that $\sigma^2(m_{iz}) = \sigma_a^2$ in this scenario as in all the others. This result is simply that observations of stars on the boresight can never improve knowledge of the misalignment component about the boresight. The y-axis attitude and misalignment variances are the same as scenario 3 with σ_m^2 being replaced by (1/2) σ_m^2, reflecting the presence of twice as many measurements. Thus

$$\sigma^2(\Delta\theta_y) = \frac{1}{2}\left(\sigma_a^2 + \frac{1}{2}\sigma_m^2\right)$$

The y-axis misalignment uncertainties are the same as those in scenario 2, using scalar observations formed from the same measurements. The new feature of scenario 4 is the coupling of $\Delta\theta_x$, $\Delta\theta_z$, m_{1x}, and m_{2x} in the 4 x 4 block in the upper-left corner of W'_n. Inverting this submatrix gives the variances

$$\sigma^2(\Delta\theta_x) = \sigma^2(\Delta\theta_z) = \sigma_m^2 \left(\frac{\sigma_m^2 + 2\,\sigma_a^2}{2\,\sigma_m^2 + 2\,\sigma_a^2} \right)$$

$$\sigma^2(m_{ix}) = (\sigma_a^{-2} + \sigma_m^{-2})^{-1}$$

The x-axis misalignment variance of the FHST is the harmonic mean of the measurement variance and the a priori alignment variance. It is, therefore, less than either variance and approaches the smaller of the two in the limit that the other becomes very large. The limits of the x- and z-axis attitude variances are (1/2) σ_m^2 for $\sigma_m \gg \sigma_a$ and σ_m^2 for $\sigma_m \ll \sigma_a$. The latter is, like $\sigma^2(m_{ix})$, finite as σ_a tends to infinity. Thus, unlike any other scenario considered, the attitude and alignment knowledge obtained from the FHSTs is much better than the a priori knowledge of the misalignments.

THEORETICAL EVALUATION SUMMARY

Table 1 summarizes the alignment variance results for the four scenarios. As the table shows, the only significant difference in the alignment variance results between the attitude-independent and the attitude-dependent methods is due to the attitude maneuver.

Table 1. Alignment Variance Results Summary

	$\sigma^2(m_{ix})$	$\sigma^2(m_{iy})$	$\sigma^2(m_{iz})$
Scenario 1	σ_a^2	$\sigma_a^2 \left(\frac{\sigma_m^2 + 1/2\,\sigma_a^2}{\sigma_m^2 + \sigma_a^2} \right)$	σ_a^2
Scenario 2	σ_a^2	$\sigma_a^2 \left(\frac{\sigma_m^2 + \sigma_a^2}{\sigma_m^2 + 2\,\sigma_a^2} \right)$	σ_a^2
Scenario 3	σ_a^2	$\sigma_a^2 \left(\frac{\sigma_m^2 + 1/2\,\sigma_a^2}{\sigma_m^2 + \sigma_a^2} \right)$	σ_a^2
Scenario 4	$(\sigma_a^{-2} + \sigma_m^{-2})^{-1}$	$\sigma_a^2 \left(\frac{\sigma_m^2 + \sigma_a^2}{\sigma_m^2 + 2\,\sigma_a^2} \right)$	σ_a^2

3. A NUMERICAL EXAMPLE

This section presents a numerical example of the results obtained in Section 2. The spacecraft that will be used in this example is EUVE, an astronomical satellite that is scheduled to launch in August 1991. Its primary attitude sensors are two FHSTs and three-axis gyroscopes. During the first 6 months, EUVE will perform a full-sky ultraviolet survey and will be spinning at rate of three revolutions per orbit around the spacecraft x-axis. After this survey phase, the spacecraft will be held at constant attitudes to measure the spectrum of various targets. The mission profile of EUVE, therefore, provides the opportunity of FHST alignment calibration under both maneuvering and stationary conditions. Although the alignment and attitude motion of EUVE differs from the analytical model presented in Section 2, they are sufficiently similar to substantiate the analytical results.

NUMERICAL MODEL

The two EUVE FHSTs are NASA standard star trackers with an 8-by-8 deg field-of-view (FOV). Their alignment is given as a 3-2-3 Euler rotation sequence. The rotation angles are given in Table 2.

Table 2. Nominal FHST Alignments

Sensor	Rotation Angles (Degrees)		
	θ_1	θ_2	θ_3
FHST-1	59.90	105.60	0.0
FHST-2	128.10	105.60	0.0

The assumed a priori alignment uncertainties are 2.68×10^{-4} radians (55.3 arc-seconds) (3σ) for each FHST axis. The measurement noise assumed is 1.944×10^{-4} radians (40.1 arc-seconds) (3σ). In the attitude-dependent case, the a priori attitude uncertainties are assumed to be 1 deg (3σ) for each axis. The measurement rate for the EUVE FHSTs is one observation per 0.256 seconds. To simplify the interpretation of the results, the gyroscopes are assumed to be perfect.

The attitude-independent alignment accuracy estimate is made using a program that implements the equations for the alignment covariance given in References 1 and 2. The attitude-dependent alignment accuracy estimate is performed using the Attitude Determination Error Analysis System (ADEAS), as described in Reference 5. In both cases, a one-orbit simulation is run. Although the sensor coverage is not continuous because a realistic star catalog is used, the length of the simulation run and the data rate are sufficient to give several thousand observations.

RESULTS

The results for the four simulation runs corresponding to the four scenarios are given in Table 3. For simplicity, the arithmetic mean of the uncertainties for the two FHSTs are given. The actual differences are in all cases less than 1 percent. All values are three-sigma.

Table 3. EUVE Alignment Uncertainties

Axis	Attitude-Independent, Nonrotating (Scenario 1)	Attitude-Independent, Rotating (Scenario 2)	Attitude-Dependent, Nonrotating (Scenario 3)	Attitude-Dependent, Rotating (Scenario 4)
X	1.94×10^{-4} (40.0)	1.90×10^{-4} (39.2)	1.93×10^{-4} (39.8)	0.32×10^{-4} (6.52)
Y	2.65×10^{-4} (54.7)	2.03×10^{-4} (41.8)	2.66×10^{-4} (54.8)	1.50×10^{-4} (30.9)
Z	2.68×10^{-4} (55.3)	2.07×10^{-4} (42.6)	2.68×10^{-4} (55.3)	1.17×10^{-4} (24.1)

NOTE: Values are in radians (arc-seconds).

OBSERVATIONS

Overall, the results in Table 3 and Section 2 agree. The smallest uncertainties are in the case of using an attitude-dependent alignment method during a maneuver. The differences between the results presented in Table 3 and the results from Section 2 are mainly due to the different geometry of the two cases. Figure 1 shows the fundamental geometry of the analytical and numerical models.

Analytical model

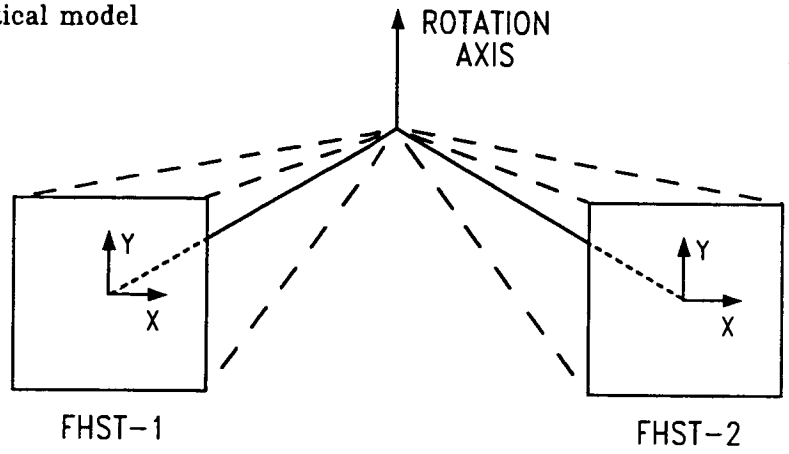

Numerical model

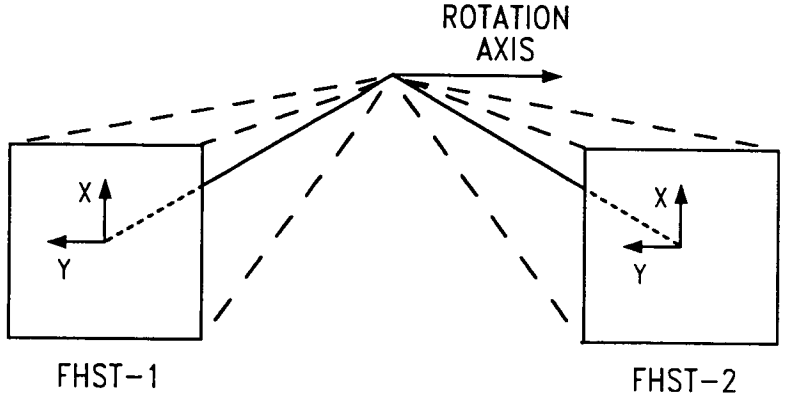

Figure 1. Geometry of the Analytical and Numerical Models

In the analytical model, a rotation about the FHST y-axis is equivalent to a change in the angle between the sensors. The corresponding axis in the numerical model is the x-axis. Table 1 indicates that the uncertainty of this axis should be 1.90×10^{-4} radians (39.1 arc-seconds). This result is in very good agreement with the first three cases. Allowing for the difference in sensor coordinate definition, the uncertainties of the y- and z-axes for the two nonrotating cases are also in good agreement with Table 1 expected results. The smaller uncertainties in the rotating cases are due to the finite FHST FOV size in the numerical example. In the nonrotating cases, the FHST observes the same star for the entire simulation. Under this condition, the y- and z-axes alignments are unobservable. This unobservability is also the consequence of assuming the star to be on the boresight as in the analytical evaluation. In the rotating numerical examples, however, the realistic star catalog used results in star measurements over the whole FOV and the alignments of the y- and z-axes are, therefore, observable. The variances of all three axes alignments in the attitude-independent case are larger than $(1/2)\ \sigma_a^2$.

4. CONCLUSION

The reason for the superior performance in the fourth measurement scenario of Section 2 is that the axis of the 90-deg attitude maneuver has been assumed to coincide exactly with the spacecraft y-axis. Since an actual estimator would obtain the angular rotation from a set of rate-integrating gyroscopes, this assumption is equivalent to the definition that the gyroscope axes are perfectly aligned with the spacecraft body axes. An overall rotation of all the sensors, including unspecified payload instruments, is indistinguishable from a spacecraft attitude rotation. Because of this perfect correlation, if the sensors and payload instruments can be coaligned, the freedom exists to arbitrarily choose one sensor to be perfectly aligned, which is equivalent to defining the spacecraft body axes in terms of this sensor's axes. The attitude-dependent algorithm, as modeled in Section 2, implicitly defines the spacecraft axes in relation to the gyroscope axes, so the improved alignments of the FHSTs in scenario 4 are actually owing to their alignment with respect to the rotation vector as measured by the gyroscopes.

An estimator that uses scalar observations as in Section 2 to align the attitude sensors does not include any attitude information. There is, therefore,

no measurement of the sensor alignment with respect to perfectly aligned gyroscopes. Because of the correlation between an overall sensor rotation and the attitude, there are three degrees of freedom in the sensor alignment that are unobservable. The resulting uncertainties in the alignment estimates, therefore, cannot be made arbitrarily small and will strongly depend on the prelaunch measurements. If the alignment uncertainty of one of the sensors is assumed to be zero, this sensor would become a reference sensor similar to the gyroscope in the attitude-dependent model. The alignment uncertainty of the other sensor should then be similar to the attitude-dependent results. To illustrate this effect, the scalar observation simulation software was executed assuming one of the sensors to be perfectly aligned. The results of this simulation are given in Table 4. Also given in Table 4 is the attitude-dependent, rotating case results from Section 3 for comparison. All values are three-sigma.

Table 4. EUVE Alignment Uncertainties Showing Reference Sensor Case Results

Axis	Attitude-Dependent, Rotating (Scenario 4)	Attitude-Independent, Rotating Reference Sensor
X	0.32×10^{-4} (6.52)	0.30×10^{-4} (6.19)
Y	1.50×10^{-4} (30.9)	1.32×10^{-4} (27.2)
Z	1.17×10^{-4} (24.1)	1.50×10^{-4} (31.0)

NOTE: Values are in radians (arc-seconds).

It can be seen that the two cases are in good agreement. This result would indicate that the distinguishing factor for producing small alignment uncertainties is not attitude-dependence or -independence but whether there is a reference sensor that serves to define an on-orbit spacecraft coordinate frame.

Whether, for a particular mission, an alignment algorithm that defines an on-orbit spacecraft frame or one that maintains the prelaunch frame should be

used depends on the type of payload. When the payload can align itself with respect to the attitude sensors, there is no need to maintain the prelaunch spacecraft reference. The ambiguity of the attitude reference can be removed by defining a new on-orbit reference, e. g., the gyroscope axes, and much improved attitude accuracies can result. However, when the payload is attitude sensitive but not sufficiently so to allow coalignment, an algorithm that preserves the prelaunch frame is preferable. In this case, the alignment of the payload is known relative only to the prelaunch reference. A method that does not make use of a reference sensor minimizes the deviation of the on-orbit sensor alignment from the prelaunch measurement and, therefore, will result in the best estimate of the payload attitude.

REFERENCES

1. Shuster, M. D., Chitre, D. M., and Niebur, D. P.,"In-Flight Estimation of Spacecraft Attitude Sensor Accuracies and Alignments," *Journal of Guidance and Control*, Vol. 5, No. 4, pp 339-343, 1982

2. Bierman, G. J. and Shuster, M. D., "Spacecraft Alignment Estimation," 27th IEEE Conference on Decision and Control, 1988

3. Markley, F. L., Seidewitz, E., and Nicholson, M., "A General Model for Attitude Determination Error Analysis," Flight Mechanics/Estimation Theory Symposium 1988, NASA Conference Publication 3011, 1988

4. Markley, F. L., Seidewitz, E., and Deutschmann, J., "Attitude Determination Error Analysis: General Model and Specific Application," presented at the CNES International Symposium on Space Dynamics, Toulouse, France, 1989

5. Nicholson, M., Markley, F. L., and Seidewitz, E., Attitude Determination Error Analysis System (ADEAS) Mathematical Specifications Document, Computer Sciences Corporation, CSC/TM-88/6001, October 1988